Numerical Model of Cloud-to-Ground Lightning for PyroCb Thunderstorms

Surajit Das Barman, Rakibuzzaman Shah, *Member, IEEE*, Syed Islam, *Life Fellow, IEEE*, and Apurv Kumar

***Abstract*—This paper demonstrates a 2-D numerical model to represent two conceptual pyrocumulonimbus (pyroCb) thundercloud structures: i) tilted dipole and ii) tripole structure with enhanced lower positive charge layer, which are hypothesized to explain the occurrence of lightning flashes in pyroCb storms created from severe wildfire events. The presented model considers more realistic thundercloud charge structures to investigate the electrical states and determine surface charge density for identifying potential lightning strike areas on Earth. Simulation results on dipole structure-based pyroCb thunderclouds confirm that the wind-shear extension of its upper positive (UP) charge layer by 2–8 km reduces the electric field and indicates the initiation of negative surface charge density around the earth periphery underneath the anvil cloud. These corresponding lateral extensions have confined the probable striking zone of –CG and +CG lightning within 0–23.5 km and 23.5–30 km in the simulation domain. In contrast, pyroCb thundercloud possessing the tripole structure with enhanced lower positive charge develops a negative electric field at the cloud's bottom part to block the progression of downward negative leader and cause the surface charge density beneath the thundercloud to become negative, which would lead to the formation of +CG flashes. Later, a parametric study is conducted assuming a positive linear correlation between the charge density and aerosol concentration to examine the effect of high aerosol concentration on surface charge density in both pyroCb thunderclouds. The proposed model can be expanded into 3-D to simulate lightning leader movement, aiding wildfire risk management.**

***Index Terms*—Cloud-to-ground lightning, long continuous current, pyrocumulonimbus, surface charge density, wind-shear extension.**

I. Introduction

WILDFIRES and other prescribed burning events generate smoke that is elevated in the updraft and propagates through conduction, convection, and radiation mechanisms [1]. During this phenomenon, the rising hot air becomes negatively buoyant while entering within the upper troposphere lower stratosphere (UTLS) region and becomes saturated via cooling from adiabatic expansion to generate dense cumuli-form clouds called pyrocumulonimbus (pyroCb) thunderclouds [2], [3]. During the formation of pyroCb events, smoke-generated aerosol particles act as a part of cloud condensation nuclei (CCN), which generally affect the progression of a thunderstorm. Like other conventional thunderstorms, pyroCb storms have large impacts on the fire behavior, formation of ice, and precipitation and often turn severe by forming hail storms or tornadoes [4]. The most significant consequence of pyroCb events is the ignition of new spot fires by cloud-to-ground (CG) lightning. PyroCb thunderclouds can give rise to the occurrence of both positive cloud-to-ground (+CG) and negative cloud-to-ground (–CG) lightning in which +CG is considered to most likely ignite secondary bushfires and cause massive damage to nature and infrastructure [1], [3], [5].

More than 90% of all flashes are negative, common in thunderstorms that develop in moist environments. On the other hand, +CG flashes are reported to be frequently developed in the dry environment with higher cloud bases [6] and in thunderstorms like pyroCb that inject huge smoke into the upper troposphere [3], [4], [7], [8], [9]. As the cloud reaches higher altitudes, the updrafts become strong, and push smoke particles and ash further upwards that can reach up to the lower stratosphere. The injection of smoke into the stratosphere region is extremely concerning because of its long-running impacts on the climate. The authors in [9] also demonstrate that storms characterized by predominantly +CG lightning activity are attributable to the presence of relatively shallower warm cloud depths. Numerous studies on +CG have exhibited its characteristics containing long continuous current (LCC), its close relation to large scale electrical-discharges and supremacy during the storm's dissipating stage, and carrying high peak current compared to –CG which boosts the risk of igniting additional wildfires [1], [5], [10], [11], [12], [13], [14]. But recent studies stipulate that –CG strokes with LCC probably could start most of the fires [15], [16], [17], [18]. According to the study conducted by Schultz et al. in 2019 [15], it was found that approximately 90% of lightning ignitions witnessed in the US from 2012 to 2015 were initiated by negative CG flashes. PyroCb lightning ignited the secondary fire is now a serious concern for firefighting management globally. Despite the increased number in the literature, only a handful of recent studies on pyroCb occurrences have been done. Over the period 1973–2014, lightning-ignited wildfire was responsible for burning 70% of land in Victoria, Australia, despite accounting for only 11% of total ignitions [19]. Several devastating wildfires occurred in the southeastern part of Australia where recent events documented as the Black Saturday, 2009 (Victoria) and Black Summer, 2019–2020 (New South Wales) initiated several distinct pyroCb

Manuscript received 17 May 2023; revised 27 July 2023; accepted 28 August 2023. Date of publication 8 September 2023; date of current version 27 September 2023. This work was supported by the Centre of New Transition Research, Federation University Australia and the Destination Australia scholarship. *(Corresponding author: Apurv Kumar.)*

The authors are with the Centre of New Energy Transition Research, Federation University Australia, Mt Helen, VIC 3353, Australia (e-mail: surajit dasbarman@students.federation.edu.au; m.shah@federation.edu.au; s.islam@federation.edu.au; apurv.kumar@federation.edu.au).

Digital Object Identifier 10.1109/JSTARS.2023.3313263

storms from multiple fire plumes and produced a large number of lightning strikes that started secondary fires [20], [21]. In 2021, numerous pyroCb clouds were observed over the wildfires that flamed across British Columbia, Canada, worsened by multiple days of record temperatures and dry weather. Burrows and Kochtubajda [22], [23] have made a detailed analysis of the electrical characteristics of about 23.5 million CG flashes detected through lightning detection networks across Canada over a decade from 1999 to 2008. During June–August 2013, 88 enormous wildfires were observed in Western North America, producing 26 intense pyroCb storms [24]. One of the biggest wildfires in the history of California was reported to burn around 104 000 ha of land and created two intense pyroCb events [25].

Diverse investigations have shown that analysis of the electric condition that favors the occurrence of LCC lightning flashes could be an essential benchmark of certain phenomena related to pyroCb events. The gross charge structure of thunderstorms develops in a moist environment, leading to the initiation of –CG flashes made up of an upright tripole having layers of positive charge at both the top and below supported by a dominant middle negative charge [26]. However, severe thunderstorms developed in dry environments statistically generate more +CG lightning [27]. Numerous hypotheses have been established in the past to interpret the charge structures and scenarios leading to +CG strikes and associate thunderstorms [28], [29], [30], [31], [32]. The previous study by Brook et al. [31] revealed that the positive charge at the top of a dipole thundercloud could be laterally displaced or extended to the cloud's forward flank due to the effect of vertical upper-level wind and tilted updraft to form the tilted dipole thundercloud, and can originate +CG lightning to the ground. Another study in [33] explained the domination of the enhanced lower positive charge layer over the middle negative charge observed in the conventional tripole thundercloud structure. The wide undiluted updrafts of the thundercloud are assumed to be the reason behind this charge configuration forming and creating +CG flashes to the ground. Still, no literature work has been reported yet on the charge structure of pyroCb thunderclouds or analysis of the electrical conditions that favour pyroCb lightning discharge. But the scenario in pyroCb storms is generally facilitated by strong wind-shear and undiluted updraft, which raise the possibility of pyroCb thunderclouds forming the charge configurations mentioned above [20], [25], [34], [35].

Two types of thundercloud modelling techniques exist to study the morphology and dynamics of lightning discharge. The first is the physical model used in past years for procuring the thundercloud structure [36], [37]. In this method, complex factors like the shape of the lightning leader tip, induced charge, and corona region must be considered to analytically simulate the actual thunderstorm physical processes and their electrical effect, particularly at the microphysical level based on the observed electric field data. However, this method is computationally expensive and cannot generate concise analytical expressions over large-scale domains. Hence, due to the long calculation time, it is difficult to identify the area on the earth's surface or any object at risk by thunder or lightning. The most popular approach to model the dynamic behavioral process of a thundercloud is to numerically analyze the coupling equation based on the given boundary value relationship [38], [39], [40], [41], [42], [43], [44]. This electrostatic concept-based numerical model represents the thundercloud in axisymmetric form, and the non-inductive charging method is mainly used to define thundercloud electrification. Despite being complex and time-consuming, this numerical modelling technique is highly effective in obtaining the dynamic change process of a thundercloud.

Many studies have demonstrated that conventional cumulonimbus clouds are highly affected by aerosols, which escalates the questions behind the effects of fire-induced aerosols on pyroCb development [45], [46], [47], [48], [49], [50]. In the case of cumulonimbus clouds, increasing aerosol loading gives rise to generating large concentrations of smaller cloud droplets which in turn reduces the collision efficiency to delay and suppress raindrop formation. Several studies have a positive correlation between lightning activity and aerosol loading [51], [52], [53]. Based on the investigation made in the works [54], [55], [56], high CCN concentration could lead to a strong electrification process under the bulk microphysical model. However, further increases in concentration weaken the electrification process. On the other hand, the role of fire-induced aerosol in the development of pyroCb thunderclouds and its electrification process still lacks solid scientific acknowledgement. The research on the potential variation of aerosol loading on pyroCb development is scarce, with only a few studies conducted so far [8], [57], [58].

This article presents a simple 2-D numerical model for two corresponding thundercloud configurations: tilted dipole structure and tripole structure having an excessively lower positive charge, which are proposed to represent pyroCb thunderclouds. The electric conditions that benefit the generation of CG flashes are analyzed through simulation. For illustrative demonstration, the charge region's position and its charge density values are continuously adjusted during the simulation. Due to the computational expenses, this modelling approach does not account for the impact of aerosol concentrations on cloud microphysics. In contrast with previous works, the proposed model considers the realistic cloud charge structures hypothesized to generate highly intense CG lightning. Based on the simulated surface charge density, it is also employed to investigate the probable lightning-striking zones underneath the pyroCb thundercloud. The proposed model shows how changes in the cloud charge structure during a pyroCb storm influence the value of the potential and electric field distribution as well as the surface charge density that could aid the development of lightning of different types. Finally, the model is used to examine the effect of aerosol concentrations on the surface charge density to get a parametric idea of the influence of smoke-induced aerosols on the electrification process in pyroCb thunderclouds.

II. Thundercloud Model Description

The primary objective of this study is to demonstrate the electrical condition that favours the occurrence of both +CG and –CG lightning from pyroCb thunderstorms and predict the probable lightning striking zone on the earth's surface. For

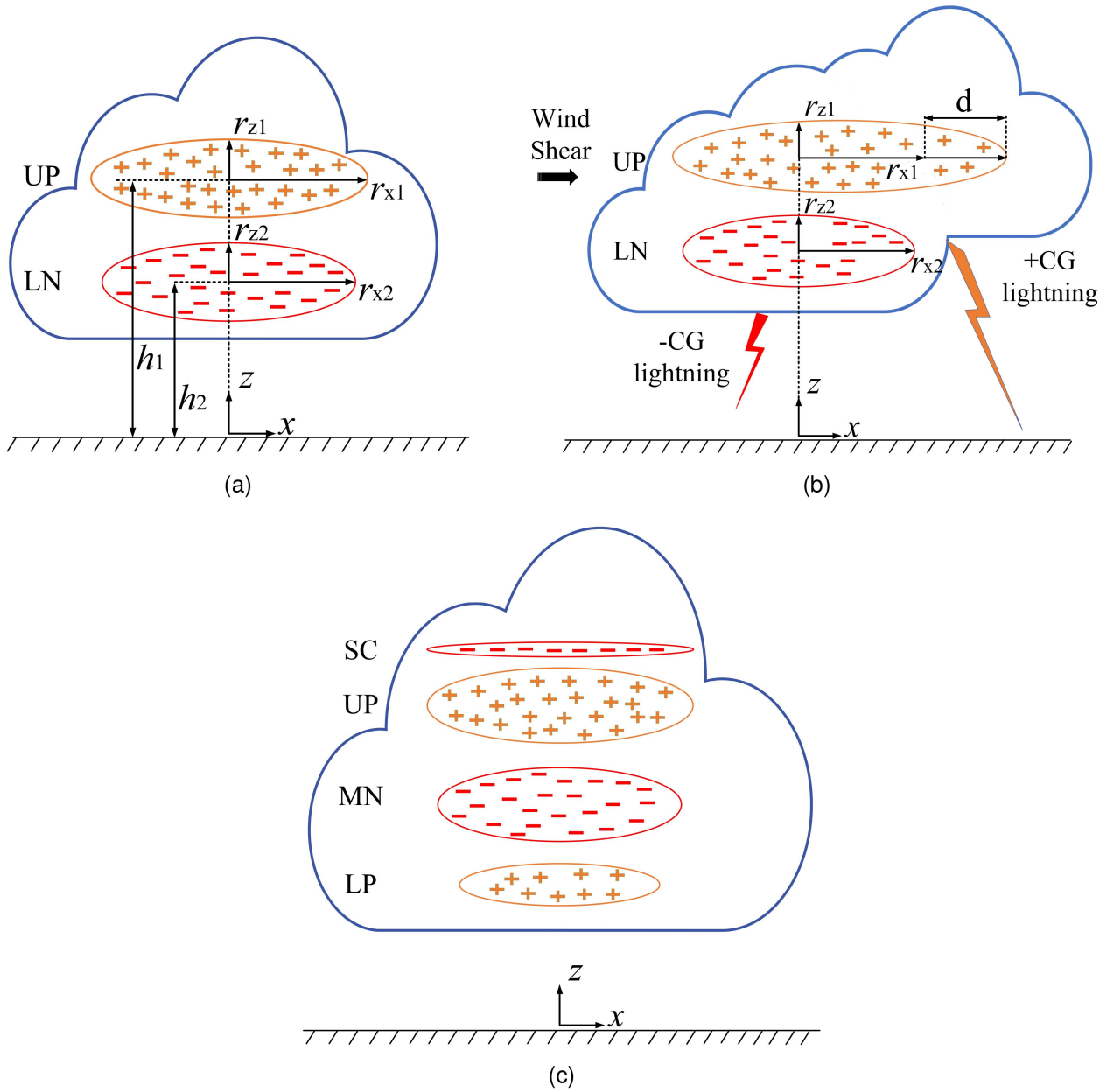

Fig. 1. Charge configurations of (a) dipole structure and (b) tilted dipole structure-based pyroCb thundercloud where UP and LN denote upper positive and lower negative charge regions, respectively; (c) pyroCb thundercloud having tripole structure consists of a dominant upper positive (UP) charge region, a dominant middle negative (MN) and a small lower positive (LP) charge regions with an additional negative screening layer (SC) at the top.

analysis, two conceptual thundercloud charge configurations - tilted dipole and conventional tripole with enhanced lower positive charge region- represent the pyroCb thunderstorms. The electrical configuration of a dipole structure-based pyroCb thundercloud can be presented with two separate charge regions: upper positive (UP) in the top and lower negative (LN) in the below forms a vertical dipole that is shown in Fig. 1(a). Typically, the charge magnitude of these two charge regions is somewhere between tens to hundreds of coulombs. Here, x and z axes represent the earth's surface underneath the cloud and the vertical range of the charge region, respectively. To simplify the calculations, the permittivity of the atmospheric region $z > 0$ is assumed to be equivalent to that of a vacuum. In the model, r_{x1} and r_{x2} denote the lateral extent of UP and LN charge regions, respectively; r_{z1} and r_{z2} represent their corresponding vertical range, and h_1 and h_2 determine their corresponding altitude. In the case of pyroCb events, strong vertical wind and titled updraft cause the lateral displacement of the UP charge in dipole structure from its LN charge centre as illustrated in Fig. 1(b). The deportation of the UP charge to the ground would result in the initiation of downward +CG strokes [31], [59]. Here, the parameter d denotes the difference between the original and current position of the extended rightward boundary of the UP charge region. For modeling, individual charge region in the dipole structure-based pyroCb thundercloud is considered to have an ellipsoidal frame with proportional charge density

TABLE I
DIMENSIONAL AND ELECTRICAL PARAMETERS OF DIPOLE STRUCTURE-BASED PYROCB THUNDERCLOUD

Charge Region	Altitude, h (km)	Lateral extent r_x (km)	Vertical extent r_z (km)	Lateral centre x_0 (km)	Peak Charge Density, $\rho(0)$ (nC/m^3)	Charge, Q (C)
UP	9.75	6	1.5	15	2.2	77
LN	6.75	5	1.5	15	-2.5	-73

distribution, which can be stated by (1) as follows.

$$\rho_n(x,z) = \rho_n(0) exp\left[\frac{(x-x_{0n})^2}{{r_{xn}}^2} + \frac{(z-h_n)^2}{{r_{zn}}^2}\right] \quad (1)$$

where $n = 1, 2, \ldots$ and $\rho_n(0)$ is the magnitude of peak charge density of nth charge region; x_{0n} acts for representing the lateral center of nth charge layer.

On the other hand, the conventional tripole thunderstorm generally consists of four main charge regions: a screening layer (SC) of negative charge at the top, upper positive (UP), middle negative (MN), and lower positive (LP) as illustrated in Fig. 1(c). This is known as the gross charge configuration of conventional thunderstorms, which causes the production of negative flashes. This tripole structure can get affected by the undiluted and extreme broad updraft during severe wildfire events characterized by its enhanced LP charge region to dominate the MN charge [33] and also affect the lightning (both +CG and –CG) striking zones on earth's surface. Similar to a tilted dipole structure, each charge region in the tripole structure-based pyroCb thundercloud is also considered to have an ellipsoid shape in this model.

The charge structures of the two conceptual pyroCb thunderclouds are modelled in 2-D cartesian coordinates, using a computational domain of 30 km × 30 km. The computational domain is discretized by keeping the distance between the neighbouring nodes equal to 500 m on both axes. The dimensional and electrical parameters of the dipole structure-based pyroCb thundercloud are provided in Table I. To simulate the effect of wind shear extension on dipole structure to the cloud's forward flank, the centre and lateral extent of UP charge are continuously adjusted while keeping its left boundary fixed. Charge in the anvil part of the cloud is assumed to have originated in the thundercloud's core and shifted towards the forward flank via lateral wind flow from the electrification region. During this process, parameter d has been varied by 0, 2, 4, 6, and 8 km while keeping the charge distribution in the UP charge region unchanged. For the tripole structure, two different cloud charge configurations are considered as summarized in Table II where the amplitude of the LP charge is increased from 18 C to 30 C as well as its corresponding lateral extent and vertical range is extended from 3 to 4 km and from 1 to 1.2 km, respectively in the 2nd configuration. According to the satellite-retrieved values, most of pyroCb's cloud-base heights averaged 3 to 5 km. These are about 7% different from the simulated value reported by in [57]. In the proposed work, the cloud-based height for two conceptual pyroCb thunderclouds can be represented by the altitude of their corresponding bottom charge layer measured from the earth's surface. The parameters for these two thundercloud structures are based on the lightning development analysis reported in [39], [40], [60].

TABLE II
DIMENSIONAL AND ELECTRICAL PARAMETERS OF TRIPOLE STRUCTURE-BASED PYROCB THUNDERCLOUD

Configuration	Charge Region	Altitude, h (km)	Lateral extent r_x (km)	Vertical extent r_z (km)	Lateral centre x_0 (km)	Peak Charge Density, $\rho(0)$ (nC/m^3)	Charge, Q (C)
1	SC	11.75	6	0.5	15	-1.1	-19
	UP	9.75	6	1.5	15	2.2	77
	MN	6.75	5	1.5	15	-2.5	-73
	LP	4.25	3	1	15	1.0	18
2	SC	11.75	6	0.5	15	-1.1	-19
	UP	9.75	6	1.5	15	2.2	77
	MN	6.75	5	1.5	15	-2.5	-73
	LP	4.25	4	1.2	15	1.5	30

During the simulation, the ground surface at $z = 0$ underneath the thundercloud is assumed to be an unbounded conducting plane with equal potential. The electric potential $V(x,z)$ generated by nth charge region in a pyroCb thundercloud specified by charge density $\rho_n(x,z)$ can be achieved via solving the Poisson equation

$$\nabla^2 V = -\frac{\rho_n(x,z)}{\epsilon_0} \quad (2)$$

Computationally, the total electric potential V for any pyroCb thundercloud structure can be represented as the addition of contributions from all discrete grid points (i,j) of the simulation domain and their corresponding images, which can be computed from the following discretized form of (2) as [61]

$$\frac{V_{i+1,j} - 2V_{i,j} + V_{i-1,j}}{\delta x^2} + \frac{V_{i,j+1} - 2V_{i,j} + V_{i,j-1}}{\delta z^2} = -\frac{1}{\epsilon_0}\sum_n \rho_n(x,z) \quad (3)$$

To enhance the convergence speed, (3) is solved with the successive over-relaxation (SOR) algorithm. The potential of the discrete node points is calculated by iterating the following (4) over the computational domain until convergent results are achieved.

$$V_{i,j}{}^{(m)} = V_{i,j}{}^{(m-1)} + \frac{\omega}{2(\delta x^2 + \delta z^2)}\left[(V_{i+1,j}{}^{(m-1)} + V_{i-1,j}{}^{(m)})\delta z^2 + (V_{i,j+1}{}^{(m-1)} + V_{i,j-1}{}^{(m)})\delta x^2 + \frac{1}{\epsilon_0}\sum_n \rho_n(x,z)\delta x^2 \delta z^2\right] \quad (4)$$

Here, the superscripts (m) and $(m-1)$ denote the corresponding current and previous iteration cycles, and the relaxation parameter ω governs the convergence speed. The electric field E in individual grid points of the computational domain can be attained from V as

$$E = -\nabla V \quad (5)$$

The charges on the earth's surface underneath any pyroCb thunderstorm are highly influenced by the charge structure built up in its thundercloud. When a thunderstorm is up above, the LN charge in the dipole structure and the dominant MN charge in the tripole structure repel negative charges on the earth's surface. It causes the earth's surface or any objects underneath the thunderstorm to become positively charged. In the case of wind-shear extension in a dipole structure-based pyroCb thundercloud, the extended UP charge contributes to building a negative charge on the earth's surface under the anvil cloud. In contrast, enhanced LP charge region in tripole structure repels positive charges on the earth's surface, which blocks the progression of downward negative leader. To obtain the surface charge on earth's surface ($z \to 0$), the negative partial derivative of the simulated value of V is taken in the direction of the normal to the surface as stated in (6). This will enable us to investigate the surface charge density σ on the earth's surface underneath the pyroCb thunderstorm.

$$\sigma = -\epsilon_o \frac{\partial}{\partial z} V \bigg|_{z=0} \tag{6}$$

III. Results and Discussion

A. Effect of Wind-Shear Extension on Dipole Structure-Based Pyrocb Thundercloud

To explore the consequence of wind-shear extension on a pyroCb thundercloud and investigate how the lateral movement of UP charge of its dipole structure affects the probable lightning striking zones, r_{x1} and x_0 of UP charge layer are varied. As exhibited in Fig. 2(a1)–(e1), the parameter d is increased by 2 km to study the effect of the wind-shear extension of UP charge region towards anvil cloud from the thunderstorm core while regulating the value of $\rho(0)$ to keep the net charge of UP constant. In this method, the value of r_{x1} of the UP charge region is increased by 1 km, respectively, adjusting its centre (value of x_0) every time. The potential generated by the pyroCb thundercloud for its tilted dipole structure and the resulting electric field distribution is analyzed and graphically depicted in Fig. 2(a2)–(e2) and Fig. 2(a3)–(e3), respectively. As observed, the magnitude of the potential contributed by the UP charge region decreases with its lateral rightward extension. This happened due to the dilution of UP charge by cloud entrainment. Also, the absolute value of the electric field in thundercloud gets lower with the increase of the extension parameter d, which satisfies the properties of the law of electrostatic field [62].

$$E_{inth}(z) = \pm 201.7 exp\left(-\frac{z}{8.4}\right). \tag{7}$$

Fig. 3(a1)–(e1) and Fig. 3(a2)–(e2) outline the potential V and electric field E_z, respectively, along the z axis measured at the core of the simulated thundercloud ($x = 15$ km) with the corresponding extension value of the UP charge. Symbols "x" in Fig. 3(a1)–(e1) represent the node point with the peak electric field where each discharge is initiated. The red dash-dotted lines in Fig. 3(a2)–(e2) refer to the initiation threshold value presented as a function of altitude expressed by (7) [63]. As observed in Fig. 3(a1)–(e1), the maximum potential shows a gradually decreasing tendency while the minimum potential increases with the gradual horizontal shifting of the UP charge layer, which in turn causes the potential point of discharge initiation to move in the negative direction. When $d = 0$ km, the potential of the lightning flash initiation point is 175.85 MV [Fig. 3(a1)]. With a gradual increase of the parameter d by 2 km, a significant variation in the potential value of flash initiation point is visible as seen in Fig. 3(b1)–(e1), and reaches around –246.5 MV when $d = 8$ km. This analysis is compatible with the result in [43], which stated that the initiation of CG lightning flashes of either polarity happens only if the potential value of the initiation point is distant beyond 0 MV. The wind-shear extension also reduces the maximum field value between UP and LN charge layers for the dipole structure-based pyroCb thundercloud [Fig. 3(a2)–(e2)]. The continuous change in the relative position between these dipole charge layers and the air conductivity and its diffusion could cause the reduction of the maximum electric field. The result is consistent with the analysis done by [64]. Fig. 3(a3)–(e3) illustrates the simulated surface charge density σ on the earth's surface for the corresponding values of d. The results of σ are presented in Table III as a function of the x axis, and the probable lightning types are identified based on the measured polarity of σ. The value of surface charge density σ over the computational domain is positive when $d = 0$ and produces a peak value of 0.3364 nC/m^2 at the centre of the dipole thundercloud as shown in Fig. 3(a3). This would generate –CG flashes within $0< x <30$ km underneath the simulated thundercloud. For the wind-shear extensions of the UP charge layer from $d = 2$ to 8 km [Fig. 3(b3)–(e3)], the possible striking zone for –CG lightning is confined between 0–23.5 km on the earth's surface and enhances the positive value of σ as well as the probability of –CG lightning strikes to the ground. Corresponding horizontal extensions of UP to the rightward direction also generate the negative value of σ within $23.5< x <30$ km in the computation domain, which can

TABLE III
Identified Probable Lightning Types for Pyrocb Thundercloud With Tilted Dipole Structure

Value of d (km)	Range of x (km)	Polarity of σ	Peak value of σ (nC/m^2)	Probable lightning types
0	$0< x <30$ km	Positive	0.3364 nC/m^2 at x = 15 km	–CG
2	$0< x \leq 23.5$ km	Positive	0.3278 nC/m^2 at x = 14.5 km	–CG
	$23.5< x <30$ km	Negative	0.0285 nC/m^2 at x = 26.5 km	+CG
4	$0< x \leq 23$ km	Positive	0.3897 nC/m^2 at x = 14.5 km	-CG
	$23< x <30$ km	Negative	0.0405 nC/m^2 at x = 26 km	+CG
6	$0< x \leq 23$ km	Positive	0.4364 nC/m^2 at x = 14 km	–CG
	$23< x <30$ km	Negative	0.0492 nC/m^2 at x = 26 km	+CG
8	$0< x \leq 23$ km	Positive	0.4787 nC/m^2 at x = 14 km	–CG
	$23< x <30$ km	Negative	0.0510 nC/m^2 at x = 26.5 km	+CG

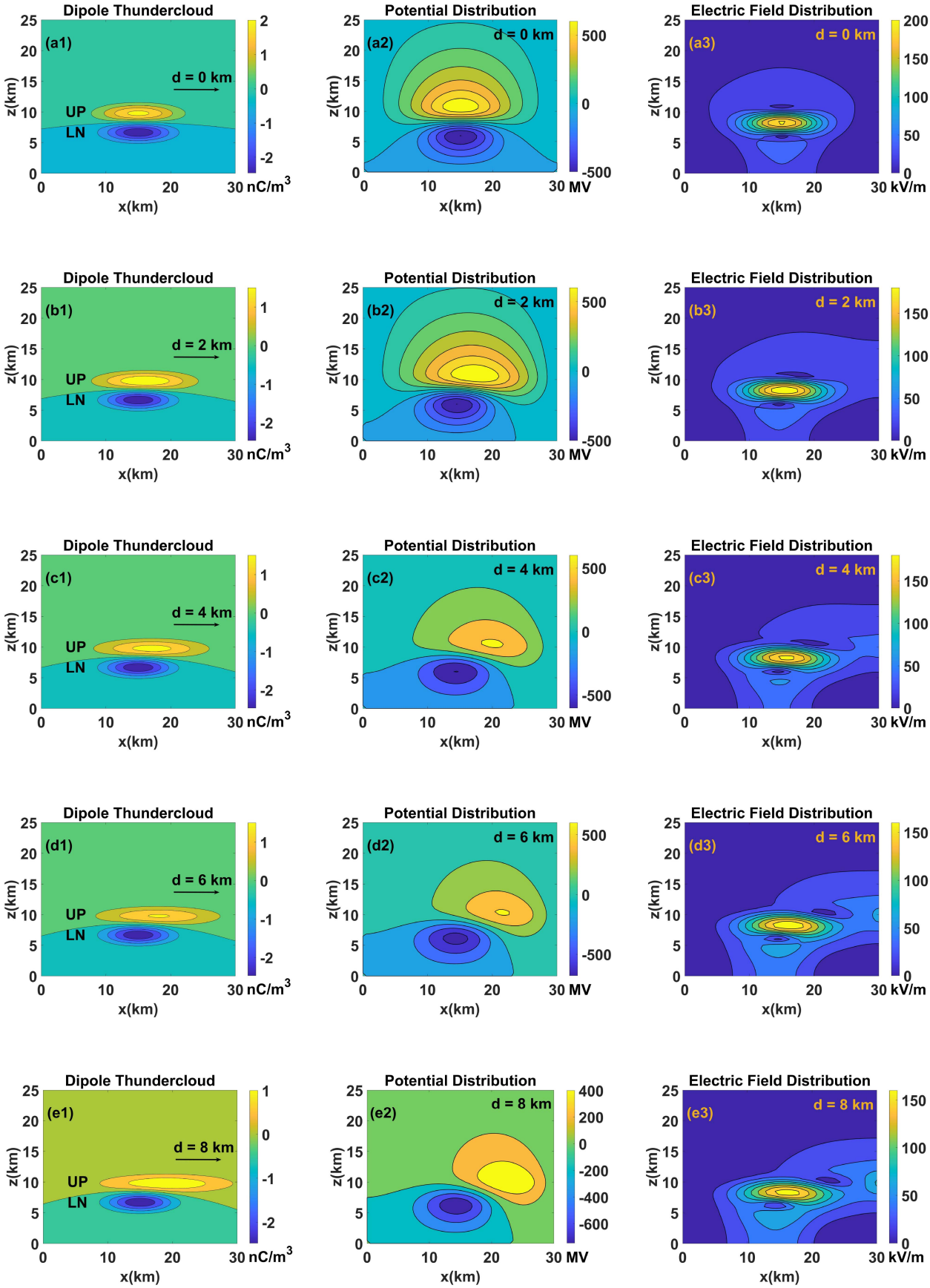

Fig. 2. Graphical projection of a dipole structure-based pyroCb thundercloud with the wind-shear extension of UP charge region when d is (a1) $d = 0$, (b1) $d = 2$, (c1) $d = 4$, (d1) $d = 6$, and (e1) $d = 8$ km, respectively; its corresponding simulated electric potential (a2-e2) and variation of the electric field (a3-e3).

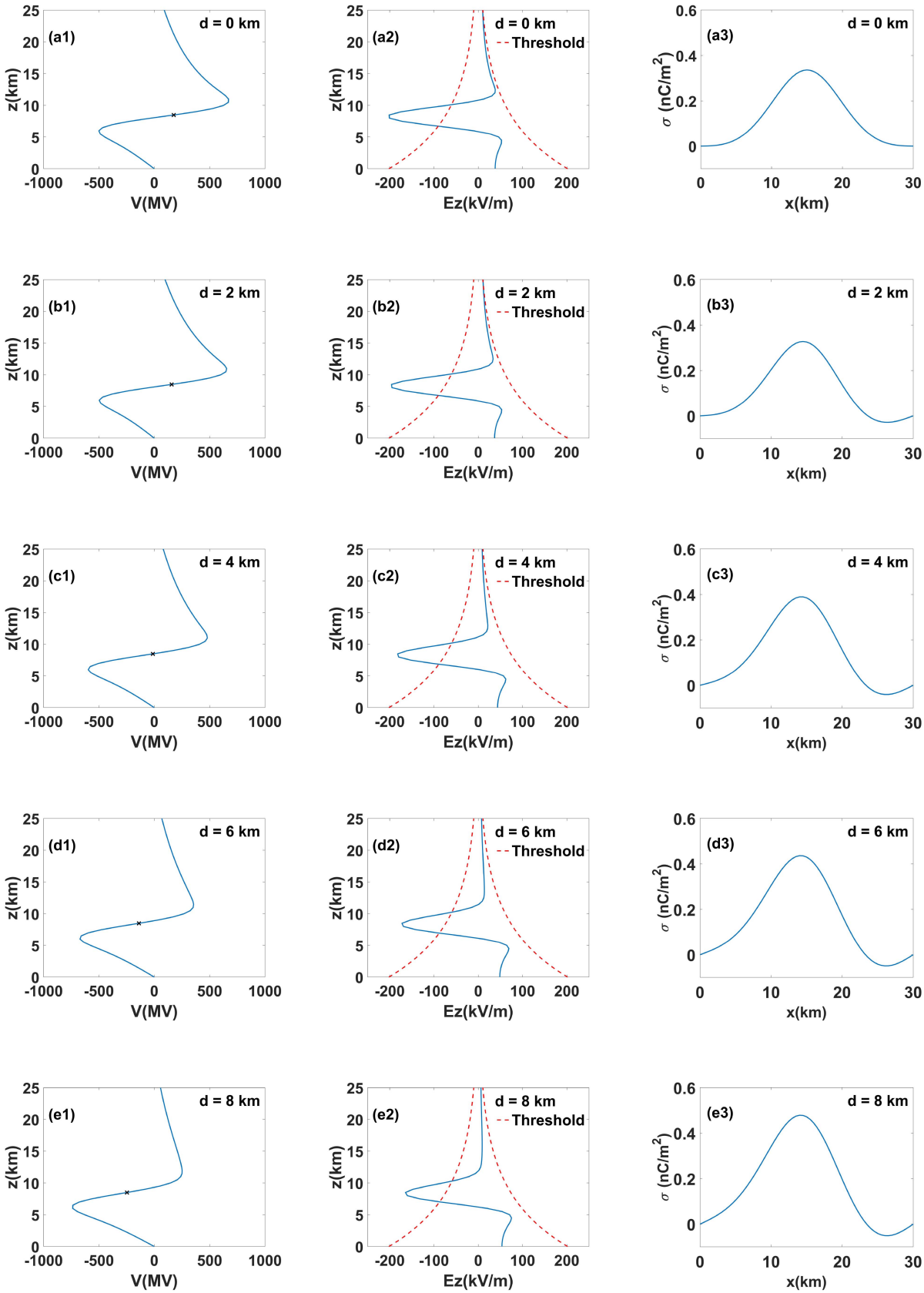

Fig. 3. Plots of the electric potential V(MV) at the maximum electric field point where the flash initiation point is denoted by the symbol "x" (a1-e1), vertical electric field E_z(kv/m) at the centre of the computational domain with its initiation threshold value is referred by red dash-dotted lines (a2-e2), and surface charge density σ underneath the dipole structure-based pyroCb thundercloud (a3-e3).

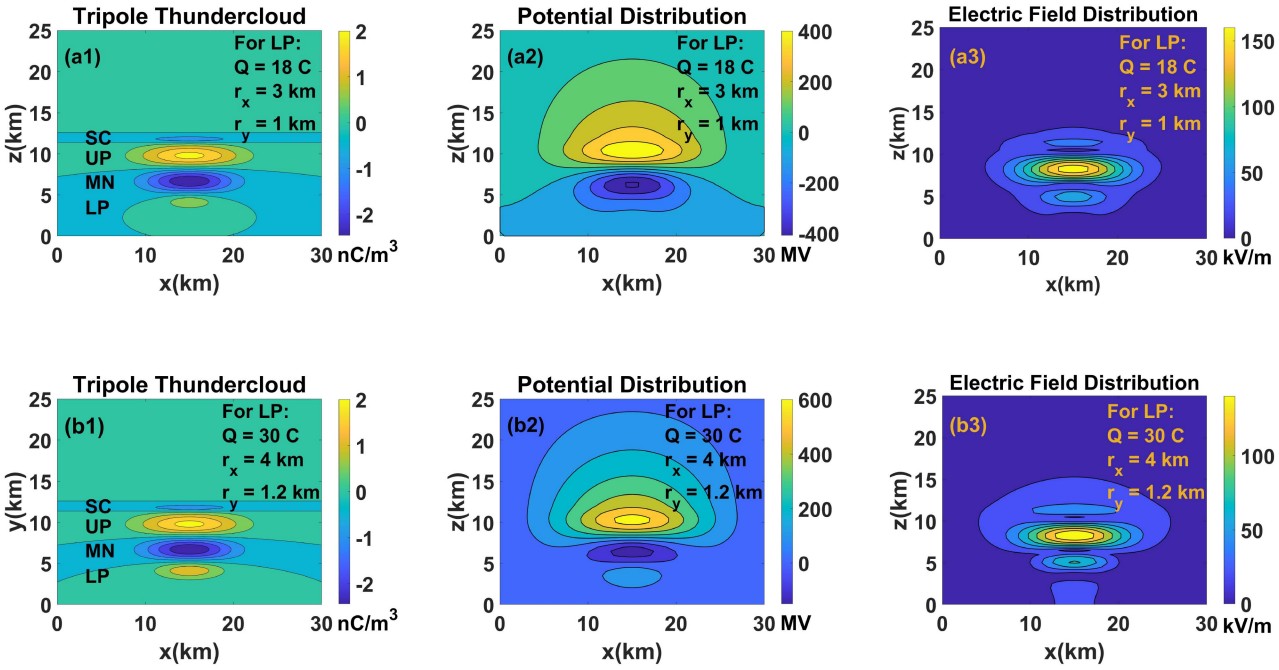

Fig. 4. Graphical projection of pyroCb thundercloud possessing tripole structure (a1) without and (b1) with enhanced LP charge region, respectively; its corresponding electric potential distribution (a2)–(b2) and variation of the electric field (a3)–(b3). In all figures, Q represents the total value of charges in the LP layer.

accelerate the occurrence of high-intensity +CG flashes in that zone. The results are consistent with the observations reported in [12] and [29] that the +CG lightning can set up extended lateral channels with stronger electric fields and typically strikes the ground far from the thundercloud core.

B. Tripole Structure-Based Pyrocb Thundercloud

Like the tilted dipole structure, a similar modeling approach is applied to represent two different configurations of the pyroCb thundercloud possessing tripole structure: without and with enhanced lower positive (LP) charge layer illustrated in Fig. 4(a1) and Fig. 4(b1), respectively. The same simulations were conducted to analyze the electric potential and field distributions for these corresponding two tripole charge configurations (highlighted in Table II) which are shown in Fig. 4(a2)–(b2) and Fig. 4(a3)–(b3), respectively. Compared to the 1st configuration of the tripole structure [Fig. 4(a2)], the total potential exhibits an overall positive growth when its LP charge region gets enhanced as observed in Fig. 4(b2). A similar rising growth is visible for the maximum potential, whereas the minimum potential shows decreasing trends while analyzing electric potential V at the maximum field point depicted in Fig. 5(a1)–(b1). As observed for the 2nd configuration, the potential point of the lightning flash initiation has taken a rightward movement with a magnitude (about 306.27 MV) 2.5 times larger than what was generated in the 1st configuration for the tripole structure-based pyroCb thundercloud. With the enhancement of the LP charge region, the vertical electric field E_z plotted in the cloud bottom becomes negative [Fig. 5(b2)], as opposed to the 1st configuration shown in Fig. 5(a2).

TABLE IV
PROBABLE LIGHTNING TYPES FOR SIMULATED PYROCB THUNDERCLOUD WITH TRIPOLE CHARGE CONFIGURATION

Lateral extent of LP (km)	Vertical extent of LP (km)	Charge of LP (C)	Range of x (km)	Polarity of σ	Peak value of σ (nC/m^2)	Probable lightning types
3	1	18	$0< x <30$ km	Positive	0.1410 nC/m^2 at x = 14 and 17 km	–CG
4	1.2	30	$0< x <30$ km	Negative	0.2080 nC/m^2 at x = 0 km	+CG

Table IV summarizes the simulation result of surface charge density σ with the probable lightning types for pyroCb thunderclouds having two different tripole charge configurations. As seen in Fig. 5(a3), σ is positive for the 1st configuration over the whole horizontal range in the simulation domain, which would lead to –CG events. This is consistent with the hypothesis explaining the presence of LP charge region under MN charge region enhances the local electric field to initiate –CG flashes [26], [65]. The same simulation was conducted to extract the value of σ for the 2nd charge configuration [Fig. 5(b3)] after extending its lateral and vertical extent as well as the charge magnitude. As observed, the value of σ in 2nd configuration becomes negative for the entire computational domain in contrast to the positive value for its 1st configuration and reaches a peak value of 0.2080 nC/m^2 at the core of the simulated pyroCb thundercloud. It would cause the development of a downward positive leader to reach the ground and lead to the formation of a +CG flash. These predicted results are compatible with the analysis done in [39] and [66], which stated that the presence

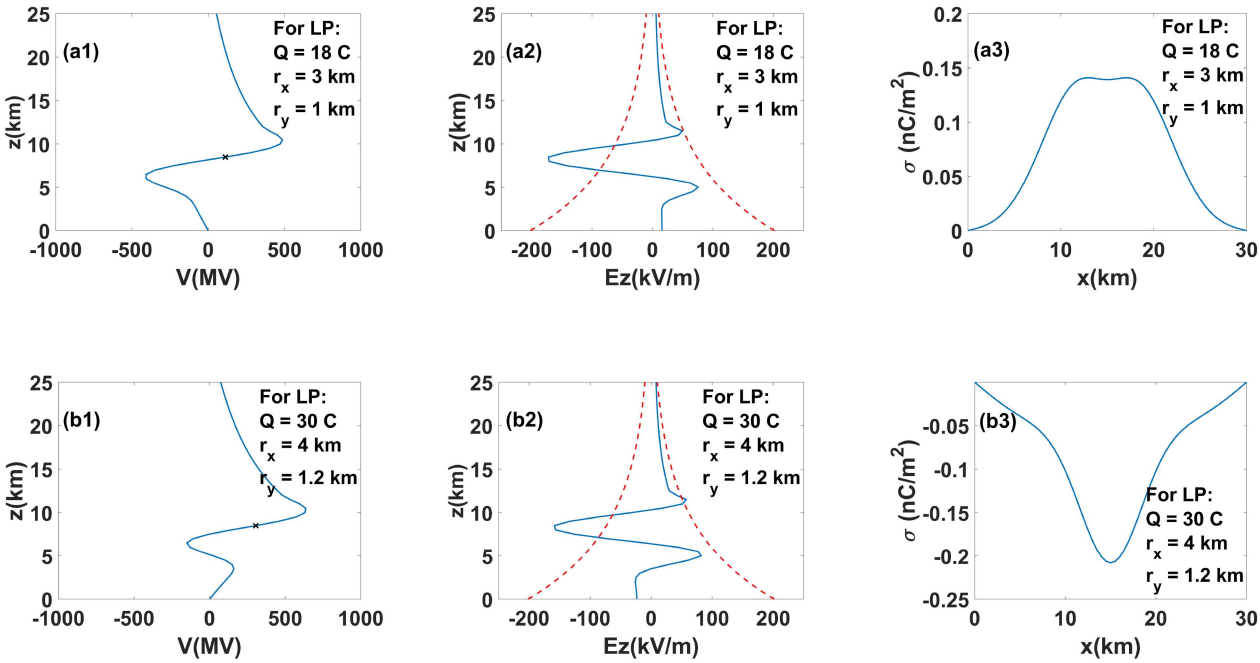

Fig. 5. Plots of electric potential V(MV) at maximum electric field point (a1-b1), electric field E_z(kV/m) at the centre along the vertical axis (a2)–(b2), and surface charge density σ (a3)–(b3) for tripole structure-based pyroCb thundercloud (a) without and (b) with enhanced LP charge region. The red dash-dotted lines in (a2)–(b2) present the threshold value of the initiation electric field.

of relatively excessive LP charge blocks the progression of downward negative leader from cloud to ground, stopping the occurrence of –CG lightning while increasing the probability of +CG flashes. This phenomenon occurs when the cloud's bottom part generates a negative electric field compared to a positive or zero.

C. Effects of Aerosol Concentration on Electrification in Pyrocb Thunderstorms

Recent observations confirm that aerosol particles are important in the cloud electrification process and lightning frequency. PyroCb thunderstorms are an exceptionally distinct category of high-base storms filled with fire-released aerosol particles. Similar to conventional thunderclouds, the presence of high aerosol concentration liberated from wildfires with strong updrafts typically delays the precipitation formation in pyroCb thunderclouds [3], [4], [5], [8]. There is no solid observational evidence of increased lightning activity at higher concentrations of aerosols for pyroCbs. The authors in [51] performed a sensitivity analysis on cumulus clouds. From the work, it is evident that a nonlinear upward trend in the peak values of both positive and negative charge densities is observed when subjected to high aerosol concentrations ($>$1 000 cm^{-3}). Consequently, this article does not aim to establish any qualitative relationship between aerosol concentration and electrification. Therefore, a positive linear correlation between the charge density and aerosol concentration for pyroCb thunderclouds is considered for the analysis. According to the observations made in [57], [67], and [68], wildfires can produce high aerosol concentrations ranging from 10 000 cm^{-3} to 20 000 cm^{-3}. To understand the impact of increasing aerosol loading, additional simulations were performed for the two conceptual pyroCb thunderclouds with six different aerosol concentration levels: N = 100, 1 000, 5 000, 10 000, 20 000, and 30 000 cm^{-3}. In dipole structure-based pyroCb thundercloud, two cases are considered to investigate the variations in surface charge density σ on the earth's surface as aerosol concentration increases. In case-I, the peak charge density of the UP charge region is linearly increased by 0.05 nC/m^2 for each 1 000 cm^{-3} increase in aerosol concentration, while for the LN charge region, it is kept constant (summarized in Table V). Fig. 6 illustrates the variations in surface charge density simulated for case-I considering the wind-shear extensions of the UP charge region by $d = 2$, 4, and 8 km, respectively. As observed in Fig. 6(a), the value of surface charge density σ approaches negative values at aerosol concentration N = 10 000 cm^{-3} and reaches the high negative peak at the periphery of the earth's surface when concentration is 30 000 cm^{-3}. When $d = 4$ and 8 km, a similar rapid growth of the negative value of σ is observed underneath the rightward extended boundary of the UP charge layer in high aerosol concentration ($\geq$20 000 cm^{-3}) shown in Fig. 6(b) and (c), respectively. For case-II, the peak charge density of the LN charge layer is also increased along with the UP charge and given in Table V. Sherwood et al. [69] have shown that elated lightning flashes are highly linked with a greater concentration of small ice particles near the upper region of cumulus clouds. In the case of high aerosol loading, more ice particles take part in the noninductive charging process, leading to large charge density [51]. This observation provides a rationale for selecting a higher enhancement rate of charge density for UP charge layers compared to LN charge in dipole structure-based pyroCb,

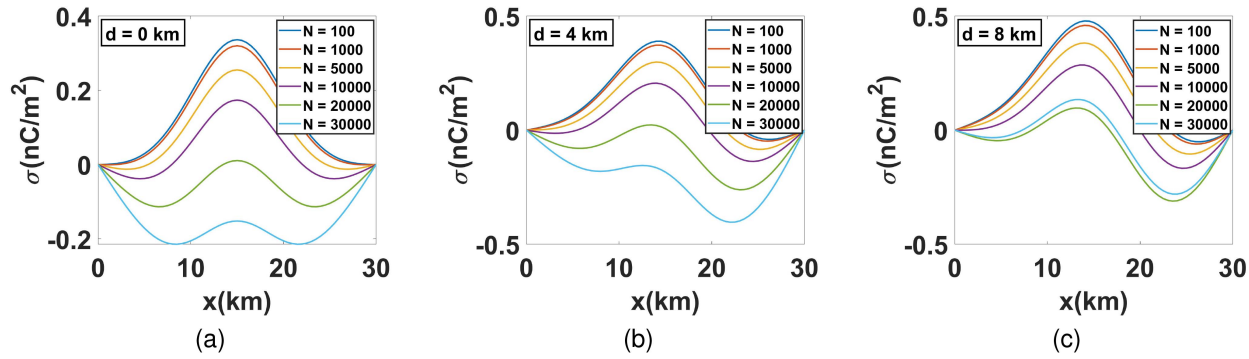

Fig. 6. Variations in surface charge density for Case-I of dipole structure-based pyroCb thundercloud when d is (a) $d = 0$, (b) $d = 4$ and (c) $d = 8$ km, respectively.

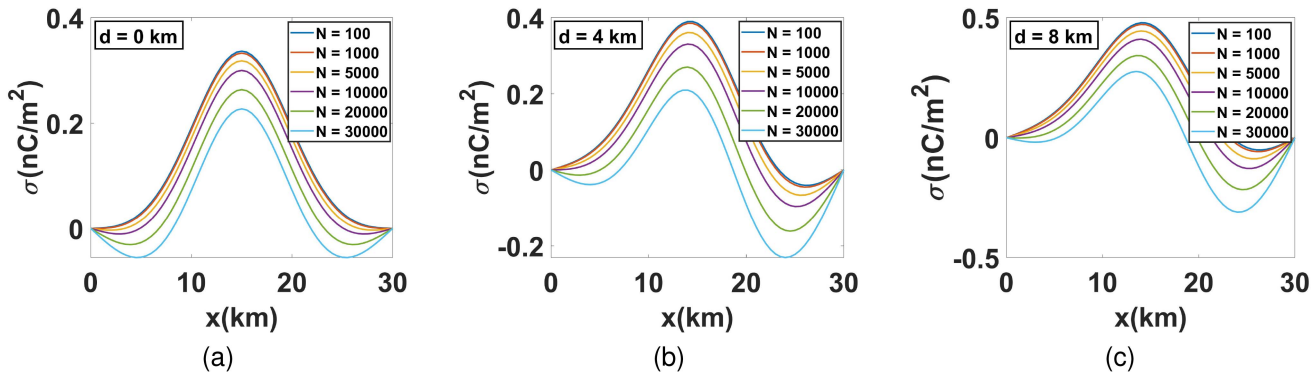

Fig. 7. Variations in surface charge density for Case-II of dipole structure-based pyroCb thundercloud when d is (a) $d = 0$, (b) $d = 4$, and (c) $d = 8$ km, respectively.

TABLE V
ENHANCEMENT RATE OF PEAK CHARGE DENSITIES OF TWO CHARGE REGIONS IN DIPOLE STRUCTURE-BASED PYROCB THUNDERCLOUD

Cloud structure	Mode	Charge region	Peak charge density at N=100 cm^{-3}	Enhancement rate of charge density per 1000 cm^{-3} rise of concentration
Dipole	I	UP	2.2 nC/m^2	0.05 nC/m^2
		LN	–2.5 nC/m^2	Constant
	II	UP	2.2 nC/m^2	0.05 nC/m^2
		LN	–2.5 nC/m^2	0.03 nC/m^2
Tripole	—	SC	–1.1 nC/m^2	Constant
		UP	2.2 nC/m^2	Constant
		MN	–2.5 nC/m^2	0.03 nC/m^2
		UP	1.0 nC/m^2	0.03 nC/m^2

especially as the aerosol concentration increases. The variations in the value of surface charge density σ for Case-II are shown in Fig. 7. In this case, σ also becomes highly negative for three corresponding values of d for concentration N is $\geq$20 000 cm^{-3}. This result demonstrates that a large background level of aerosol concentrations increases the probability of +CG lightning striking far from the pyroCb thundercloud base while possessing the titled dipole charge structure.

PyroCb thunderclouds are generally facilitated by strong undiluted updrafts, which raise the high probability of possessing the tripole charge structure having a large lower positive charge region that forms in the initial stage of the storm. The detailed analysis of the effect of increasing the charge density of the LP charge region on electrical states inside the tripole structure and the resulting negative surface charge density to produce +CG flashes has been described in the previous section. To observe the effect of increasing aerosol concentration on tripole structure-based pyroCb thundercloud, this article considers a similar enhancement rate of the charge density for both MN and LP charge regions (Table V). Fig. 8 shows the simulated surface charge density change σ. The value of σ remains positive with rapid growth after the aerosol concentration higher than 5 000 cm^{-3}, enhancing the –CG lightning striking probability. Overall, extreme wildfires that produce enormous smoke aerosols can increase the probability of both +CG and –CG lightning, depending on the charge structure and the modification of charge densities based on aerosol concentration in pyroCb thunderclouds.

In summary, the purpose of this study is to numerically represent two different thundercloud structures hypothesized for highly intense lightning strikes in severe storms like pyroCb events. Using the model, simulation results showed how changes in pyroCb thundercloud structure affect the potential distribution

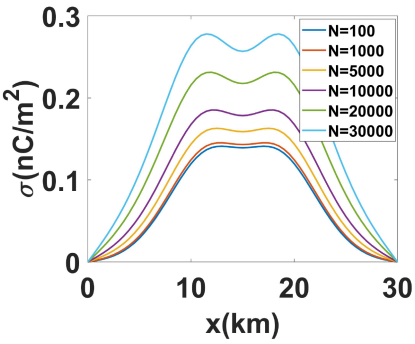

Fig. 8. Variations in surface charge density for tripole structure-based pyroCb thundercloud considering high aerosol concentration enhance charge densities of MN and LP charge regions.

and its longitudinal electric field. The results measure the surface charge density beneath thunderclouds for estimating the approximate lightning striking zone on the earth's surface. For dipole structure-based pyroCb thunderclouds, the flash initiation point moves in the negative direction with the wind-shear extension of the UP charge to reduce the maximum field value between the dipole charge layers. A negative peak value of surface charge density is found on the earth's surface just underneath the anvil cloud part, and +CG lightning could strike on that zone away from the thundercloud core. In contrast, the flash initiation point has moved in a rightward direction for the tripole structure-based pyroCb thundercloud when its LP charge region gets large and the negative value of surface charge density reaches a peak just underneath the thundercloud and can ignite +CG flashes to the earth's surface zone close to the storm's core. Besides, wildfire-generated aerosol concentration can significantly influence pyroCb lightning activities. A parametric investigation has been carried out on the impact of elevated aerosol concentration on surface charge density, assuming a positive linear correlation between the charge density and aerosol concentration for both pyroCb thundercloud structures. Study shows that the occurrence of both +CG and –CG lightning strikes can be highly influenced by the charge structure and changes in charge densities due to varying aerosol concentrations within pyroCb thunderclouds. Benefiting from short computing time, this concise thundercloud model could be useful for assuring early warning or protection, especially against wildfire-generated lightning events.

IV. Conclusion

PyroCb thunderclouds produced from extreme wildfires can generate lightning flashes to ignite further spot fires, making the storm last longer. Lightning-caused secondary fires are a serious concern for fire-fighting management as they are responsible for notable losses of lives and infrastructures globally. Detecting and controlling lightning-induced fires can be difficult due to their frequent occurrence in remote and regional areas, especially for countries with a larger geographical area. This article demonstrates a simple numerical model constructed in 2-D for two realistic cloud charge configurations: Tilted dipole and tripole structures proposed to portray pyroCb thunderclouds to identify the probable lightning striking zones on the earth's surface. The thundercloud model is developed by numerically solving Poisson's equation using the relaxation method. The variations in the value of the flash initiation point and the potential distribution and electric field for both pyroCbs are analyzed and explained in how they affect the charge density value on the earth's surface. For 2 to 8 km of wind-shear extension of the upper positive charge region of the tilted dipole structure, the potential value shows a decreasing trend that reduces the electric field between the dipole charge layers and the probable striking zone for –CG lightning is confined between $d = 0$–23.5 km within the computational domain following with the increased magnitude of positive surface charge density. Variation in the relative position between the dipole charge layers causes negative surface charge density within the 23.5 to 30 km range underneath the anvil thundercloud, which could be affected by +CG strikes. For the pyroCb thundercloud hold tripole structure with enhanced lower positive charge region, a positive growth of electric potential is observed, which causes the surface charge density to turn negative for the total computational domain and could initiate +CG flashes. Also, a parametric study examines how wildfire-generated elevated aerosol concentration affects surface charge density on the earth's surface in pyroCb thunderclouds. The study assumes a positive linear relationship between charge density and aerosol concentration, raising the likelihood of both +CG and –CG lightning. Such a model would serve as the foundation to identify areas at high risk of lightning strikes during severe weather events like pyroCb storms. Analyzing the simulated surface charge density data would provide valuable information for assessing vulnerable areas and issuing early warnings against lightning strikes. This knowledge can greatly benefit firefighting management, power network operators, critical infrastructure risk management teams, and the weather department, enabling them to understand better and anticipate the potential dangers associated with pyroCb lightning, ultimately improving safety measures and preparedness during wildfire incidents. To a greater extent, the proposed model can be modified to perform the lightning leader simulation, considering both the electric field distribution and surface charge density at the ground, to serve as the groundwork for predicting pyroCb lightning activity. This framework can also be extended into a 3-D model for a more realistic representation of severe thunderstorms formed under different weather conditions and scenarios.

References

[1] D. Latham and E. Williams, "Lightning and forest fires," in *Forest Fires*, Amsterdam, Netherlands: Elsevier, 2001, pp. 375–418.
[2] C. Ichoku, L. Giglio, M. J. Wooster, and L. A. Remer, "Global characterization of biomass-burning patterns using satellite measurements of fire radiative energy," *Remote Sens. Environ.*, vol. 112, no. 6, pp. 2950–2962, 2008.
[3] M. Fromm et al., "The untold story of pyrocumulonimbus," *Bull. Amer. Meteorol. Soc.*, vol. 91, no. 9, pp. 1193–1210, 2010.
[4] M. Fromm, R. Servranckx, B. J. Stocks, and D. A. Peterson, "Understanding the critical elements of the pyrocumulonimbus storm sparked by high-intensity wildland fire," *Commun. Earth Environ.*, vol. 3, no. 1, 2022, Art. no. 243.
[5] K. Tory and W. Thurston, *Pyrocumulonimbus: A Literature Review*. East Melbourne, VIC, Australia: Bushfire and Natural Hazards CRC, 2015.

[6] L. D. Carey and K. M. Buffalo, "Environmental control of cloud-to-ground lightning polarity in severe storms," *Monthly Weather Rev.*, vol. 135, no. 4, pp. 1327–1353, 2007.

[7] D. A. Peterson et al., "Australia's black summer pyrocumulonimbus super outbreak reveals potential for increasingly extreme stratospheric smoke events," *NPJ Climate Atmospheric Sci.*, vol. 4, no. 1, 2021, Art. no. 38.

[8] D. Rosenfeld, M. Fromm, J. Trentmann, G. Luderer, M. Andreae, and R. Servranckx, "The Chisholm firestorm: Observed microstructure, precipitation and lightning activity of a pyro-cumulonimbus," *Atmospheric Chem. Phys.*, vol. 7, no. 3, pp. 645–659, 2007.

[9] E. Williams, V. Mushtak, D. Rosenfeld, S. Goodman, and D. Boccippio, "Thermodynamic conditions favorable to superlative thunderstorm updraft, mixed phase microphysics and lightning flash rate," *Atmospheric Res.*, vol. 76, no. 1/4, pp. 288–306, 2005.

[10] P. M. Bitzer, "Global distribution and properties of continuing current in lightning," *J. Geophys. Res. Atmospheric*, vol. 122, no. 2, pp. 1033–1041, 2017.

[11] S. D. Rudlosky and H. E. Fuelberg, "Seasonal, regional, and storm-scale variability of cloud-to-ground lightning characteristics in florida," *Monthly Weather Rev.*, vol. 139, no. 6, pp. 1826–1843, 2011.

[12] V. Rakov, "A review of positive and bipolar lightning discharges," *Bull. Amer. Meteorol. Soc.*, vol. 84, no. 6, pp. 767–776, 2003.

[13] Y. Xie, K. Xu, T. Zhang, and X. Liu, "Five-year study of cloud-to-ground lightning activity in Yunnan province, China," *Atmospheric Res.*, vol. 129, pp. 49–57, 2013.

[14] Q. Zhang et al., "Characteristics and simulation of lightning current waveforms during one artificially triggered lightning," *Atmospheric Res.*, vol. 91, no. 2/4, pp. 387–392, 2009.

[15] C. J. Schultz, N. J. Nauslar, J. B. Wachter, C. R. Hain, and J. R. Bell, "Spatial, temporal and electrical characteristics of lightning in reported lightning-initiated wildfire events," *Fire*, vol. 2, no. 2, pp. 1–15, 2019.

[16] B. W. Duncan, F. W. Adrian, and E. D. Stolen, "Isolating the lightning ignition regime from a contemporary background fire regime in East-Central Florida, USA," *Can. J. Forest Res.*, vol. 40, no. 2, pp. 286–297, 2010.

[17] N. J. Nauslar, "Examining the lightning polarity of lightning caused wildfires," in *Proc. 23rd Int. Lightning Detection Conf.*, Tucson, AZ, USA, 2014, pp. 18–19.

[18] G. Wendler, J. Conner, B. Moore, M. Shulski, and M. Stuefer, "Climatology of alaskan wildfires with special emphasis on the extreme year of 2004," *Theor. Appl. Climatol.*, vol. 104, pp. 459–472, 2011.

[19] N. Read, T. J. Duff, and P. G. Taylor, "A lightning-caused wildfire ignition forecasting model for operational use," *Agricultural Forest Meteorol.*, vol. 253, pp. 233–246, 2018.

[20] A. J. Dowdy, M. D. Fromm, and N. McCarthy, "Pyrocumulonimbus lightning and fire ignition on black saturday in Southeast Australia," *J. Geophys. Res. Atmospheres*, vol. 122, no. 14, pp. 7342–7354, 2017.

[21] P. Deb et al., "Causes of the widespread 2019–2020 Australian bushfire season," *Earth's Future*, vol. 8, no. 11, 2020, Art. no. e2020EF001671.

[22] W. R. Burrows and B. Kochtubajda, "A decade of cloud-to-ground lightning in Canada: 1999–2008. Part 1: Flash density and occurrence," *Atmospheres Ocean*, vol. 48, no. 3, pp. 177–194, 2010.

[23] B. Kochtubajda and W. R. Burrows, "Cloud-to-ground lightning activity over Canada from 1999 to 2018," in *Proc. AGU Fall Meeting Abstr.*, 2019, pp. AE21A–01.

[24] D. A. Peterson, M. D. Fromm, J. E. Solbrig, E. J. Hyer, M. L. Surratt, and J. R. Campbell, "Detection and inventory of intense pyroconvection in Western North America using goes-15 daytime infrared data," *J. Appl. Meteorol. Climatol.*, vol. 56, no. 2, pp. 471–493, 2017.

[25] D. A. Peterson et al., "The 2013 rim fire: Implications for predicting extreme fire spread, pyroconvection, and smoke emissions," *Bull. Am. Meteorol. Soc.*, vol. 96, no. 2, pp. 229–247, 2015.

[26] E. R. Williams, "The tripole structure of thunderstorms," *J. Geophys. Res. Atmos.*, vol. 94, no. D11, pp. 13151–13167, 1989.

[27] R. M. Reap and D. R. MacGorman, "Cloud-to-ground lightning: Climatological characteristics and relationships to model fields, radar observations, and severe local storms," *Monthly Weather Rev.*, vol. 117, no. 3, pp. 518–535, 1989.

[28] E. R. Williams, "The electrification of thunderstorms," *Sci. Amer.*, vol. 259, no. 5, pp. 88–99, 1988.

[29] A. Nag and V. A. Rakov, "Positive lightning: An overview, new observations, and inferences," *J. Geophys. Res. Atmos.*, vol. 117, no. D8, pp. 1–20, 2012.

[30] X. Kong, Y. Zhao, T. Zhang, and H. Wang, "Optical and electrical characteristics of in-cloud discharge activity and downward leaders in positive cloud-to-ground lightning flashes," *Atmos. Res.*, vol. 160, pp. 28–38, 2015.

[31] M. Brook, M. Nakano, P. Krehbiel, and T. Takeuti, "The electrical structure of the Hokuriku winter thunderstorms," *J. Geophys. Res. Oceans*, vol. 87, no. C2, pp. 1207–1215, 1982.

[32] S. A. Tessendorf, S. A. Rutledge, and K. C. Wiens, "Radar and lightning observations of normal and inverted polarity multicellular storms from steps," *Monthly Weather Rev.*, vol. 135, no. 11, pp. 3682–3706, 2007.

[33] D. R. MacGorman and D. W. Burgess, "Positive cloud-to-ground lightning in tornadic storms and hailstorms," *Monthly Weather Rev.*, vol. 122, no. 8, pp. 1671–1697, 1994.

[34] B. E. Potter, "Atmospheric interactions with wildland fire behaviour–I. Basic surface interactions, vertical profiles and synoptic structures," *Int. J. Wildland Fire*, vol. 21, no. 7, pp. 779–801, 2012.

[35] B. E. Potter, "Atmospheric interactions with wildland fire behaviour–II. Plume and vortex dynamics," *Int. J. Wildland Fire*, vol. 21, no. 7, pp. 802–817, 2012.

[36] V. Cooray, U. Kumar, F. Rachidi, and C. A. Nucci, "On the possible variation of the lightning striking distance as assumed in the IEC lightning protection standard as a function of structure height," *Electr. Power Syst. Res.*, vol. 113, pp. 79–87, 2014.

[37] V. Mazur and L. H. Ruhnke, "Model of electric charges in thunderstorms and associated lightning," *J. Geophys. Res. Atmos.*, vol. 103, no. D18, pp. 23299–23308, 1998.

[38] T. Zheng, Y. Tan, and Y. Wang, "Numerical simulation to evaluate the effects of upward lightning discharges on thunderstorm electrical parameters," *Adv. Atmos. Sci.*, vol. 38, no. 3, pp. 446–459, 2021.

[39] D. Iudin, V. Rakov, E. Mareev, F. Iudin, A. Syssoev, and S. Davydenko, "Advanced numerical model of lightning development: Application to studying the role of LPCR in determining lightning type," *J. Geophys. Res. Atmos.*, vol. 122, no. 12, pp. 6416–6430, 2017.

[40] H. Wang, F. Guo, T. Zhao, M. Qin, and L. Zhang, "A numerical study of the positive cloud-to-ground flash from the forward flank of normal polarity thunderstorm," *Atmos. Res.*, vol. 169, pp. 183–190, 2016.

[41] E. R. Mansell, D. R. MacGorman, C. L. Ziegler, and J. M. Straka, "Simulated three-dimensional branched lightning in a numerical thunderstorm model," *J. Geophys. Res. Atmos.*, vol. 107, no. D9, pp. ACL–2, 2002.

[42] E. R. Mansell, C. L. Ziegler, and E. C. Bruning, "Simulated electrification of a small thunderstorm with two-moment bulk microphysics," *J. Atmos. Sci.*, vol. 67, no. 1, pp. 171–194, 2010.

[43] Y. Tan, S. Tao, Z. Liang, and B. Zhu, "Numerical study on relationship between lightning types and distribution of space charge and electric potential," *J. Geophys. Res. Atmos.*, vol. 119, no. 2, pp. 1003–1014, 2014.

[44] M. Hayakawa, D. Iudin, and V. Y. Trakhtengerts, "Modeling of thundercloud VHF/UHF radiation on the lightning preliminary breakdown stage," *J. Atmos. Sol. Terr. Phys.*, vol. 70, no. 13, pp. 1660–1668, 2008.

[45] W.-K. Tao, J.-P. Chen, Z. Li, C. Wang, and C. Zhang, "Impact of aerosols on convective clouds and precipitation," *Rev. Geophys.*, vol. 50, no. 2, pp. 1–62, 2012.

[46] D. Rosenfeld et al., "Flood or drought: How do aerosols affect precipitation?," *Sci.*, vol. 321, no. 5894, pp. 1309–1313, 2008.

[47] M. Shrivastava et al., "Modeling aerosols and their interactions with shallow cumuli during the 2007 chaps field study," *J. Geophys. Res.: Atmospheres*, vol. 118, no. 3, pp. 1343–1360, 2013.

[48] J. Fan, Y. Wang, D. Rosenfeld, and X. Liu, "Review of aerosol–cloud interactions: Mechanisms, significance, and challenges," *J. Atmospheric Sci.*, vol. 73, no. 11, pp. 4221–4252, 2016.

[49] T. Goren and D. Rosenfeld, "Decomposing aerosol cloud radiative effects into cloud cover, liquid water path and twomey components in marine stratocumulus," *Atmospheric Res.*, vol. 138, pp. 378–393, 2014.

[50] S. M. Saleeby, W. R. Cotton, D. Lowenthal, and J. Messina, "Aerosol impacts on the microphysical growth processes of orographic snowfall," *J. Appl. Meteorol. Climatol.*, vol. 52, no. 4, pp. 834–852, 2013.

[51] P. Zhao, Y. Yin, and H. Xiao, "The effects of aerosol on development of thunderstorm electrification: A numerical study," *Atmospheric Res.*, vol. 153, pp. 376–391, 2015.

[52] Y. Tan, L. Peng, Z. Shi, and H. Chen, "Lightning flash density in relation to aerosol over Nanjing (China)," *Atmospheric Res.*, vol. 174, pp. 1–8, 2016.

[53] S. Kar and Y. Liou, "Enhancement of cloud-to-ground lightning activity over Taipei, Taiwan in relation to urbanization," *Atmospheric Res.*, vol. 147, pp. 111–120, 2014.

[54] Y. Tan et al., "A numerical study of aerosol effects on electrification of thunderstorms," *J. Atmospheric Sol.- Terr. Phys.*, vol. 154, pp. 236–247, 2017.

[55] E. R. Mansell and C. L. Ziegler, "Aerosol effects on simulated storm electrification and precipitation in a two-moment bulk microphysics model," *J. Atmospheric Sci.*, vol. 70, no. 7, pp. 2032–2050, 2013.
[56] Y. Yang, J. Sun, F. Li, T. Zhang, W. Hu, and J. Zhang, "A numerical study of effects of aerosol particles on the electric activities of a thunderstorm with a 1.5D aerosol-cloud bin model," *J. Aerosol Sci.*, vol. 162, 2022, Art. no. 105975.
[57] S. S. Lee et al., "Examination of effects of aerosols on a pyrocb and their dependence on fire intensity and aerosol perturbation," *Atmospheric Chem. Phys.*, vol. 20, no. 6, pp. 3357–3371, 2020.
[58] G. Kablick et al., "The great slave lake pyrocb of 5 august 2014: Observations, simulations, comparisons with regular convection, and impact on UTLS water vapor," *J. Geophys. Res.: Atmospheres*, vol. 123, no. 21, pp. 12–332, 2018.
[59] Y. Yair, B. Lynn, M. Yaffe, and Y. Namia-Cohen, "Revisiting the "tilted dipole" concept for explaining the high percentage of positive ground flashes in winter thunderstorms," in *Proc. AGU Fall Meeting Abstr.*, 2019, pp. AE24A–16.
[60] K. C. Wiens, S. A. Rutledge, and S. A. Tessendorf, "The 29 june 2000 supercell observed during steps. part II: Lightning and charge structure," *J. Atmospheres Sci.*, vol. 62, no. 12, pp. 4151–4177, 2005.
[61] J. D. Hoffman and S. Frankel, *Numerical Methods for Engineers and Scientists*. Boca Raton, FL, USA: CRC Press, 2018.
[62] R. G. Powell, *Electrostatic Fields 1*. Berlin, Germany: Springer, 1990.
[63] T. C. Marshall, M. P. McCarthy, and W. D. Rust, "Electric field magnitudes and lightning initiation in thunderstorms," *J. Geophys. Res. Atmospheres*, vol. 100, no. D4, pp. 7097–7103, 1995.
[64] J. Dye et al., "Electric fields, cloud microphysics, and reflectivity in anvils of florida thunderstorms," *J. Geophys. Res. Atmospheres*, vol. 112, no. D11, pp. 1–18, 2007.
[65] A. Nag and V. A. Rakov, "Some inferences on the role of lower positive charge region in facilitating different types of lightning," *Geophys. Res. Lett.*, vol. 36, no. 5, pp. 1–5, 2009.
[66] L. Coleman, M. Stolzenburg, T. Marshall, and M. Stanley, "Horizontal lightning propagation, preliminary breakdown, and electric potential in new Mexico thunderstorms," *J. Geophys. Res. Atmospheres*, vol. 113, no. D9, pp. 1–12, 2008.
[67] J. S. Reid, P. V. Hobbs, A. L. Rangno, and D. A. Hegg, "Relationships between cloud droplet effective radius, liquid water content, and droplet concentration for warm clouds in Brazil embedded in biomass smoke," *J. Geophys. Res.: Atmospheres*, vol. 104, no. D6, pp. 6145–6153, 1999.
[68] G. Luderer, J. Trentmann, and M. O. Andreae, "A new look at the role of fire-released moisture on the dynamics of atmospheric pyro-convection," *Int. J. Wildland Fire*, vol. 18, no. 5, pp. 554–562, 2009.
[69] S. C. Sherwood, V. T. Phillips, and J. Wettlaufer, "Small ice crystals and the climatology of lightning," *Geophys. Res. Lett.*, vol. 33, no. 5, pp. 1–4, 2006.

Surajit Das Barman received the B.Sc. degree in electrical and electronic engineering from Chittagong University of Engineering and Technology, Chittagong, Bangladesh, in 2009, and the M.Sc. degree in electrical engineering from University of Malaya, Kuala Lumpur, Malaysia, in 2016. He is currently working toward the Ph.D. degree in electrical engineering with the Centre of New Energy Transition Research, Federation University Australia, Ballarat, Australia.

His research interests include wireless power transfer, numerical modeling, and renewable energy system.

Rakibuzzaman Shah (Member, IEEE) received the B.Sc. degree in electrical engineering, from Khulna University of Engineering and Technology, Khula, Bangladesh, in 2005, the M.Eng. degree in energy from the Asian Institute of Technology, Bangkok, Thailand, in 2009, and the Ph.D. degree from the University of Queensland Australia, Brisbane, Australia, in 2014. He is a Senior Lecturer in smart power systems engineering (and Research Theme Leader) with the Centre for New Energy Transition, Federation University Australia (FedUni Australia), Ballarat, Australia. Before joining FedUni Australia, he worked with the University of Manchester, Manchester, U.K., the University of Queensland, QLD, Australia, and Central Queensland University, Rockhampton, Australia. He has experience working with and consulting with DNOs and TSOs on individual projects and collaborative work on a large number of projects (EPSRC project on Multi-terminal HVDC, Scottish and Southern Energy Multi-infeed HVDC)—primarily on the dynamic impact of integrating new technologies and power electronics into large systems. He has more than 106 international publications (journals and conferences) and has spoken at the leading power system conferences worldwide. He has led projects of over 2.0 M in the last three years in the areas of his interest. His research interests include future power grids (i.e., renewable energy integration, wide-area control), asynchronous grid connection through VSC-HVDC, power system stability and dynamics, application of data mining in power system, application of control theory in power system, distribution system energy management, and low carbon energy system.

Syed Islam (Life Fellow, IEEE) received the B.Sc. degree in electrical engineering from the Bangladesh University of Engineering and Technology, Dhaka, Bangladesh, in 1979, and the M.Sc. and Ph.D. degrees in electrical power engineering from the King Fahd University of Petroleum and Minerals, Dhahran, Saudi Arabia, in 1983 and 1988, respectively.

He is currently the Dean of the School of Engineering, IT and Physical Sciences, Federation University Australia, Ballarat, VIC, Australia. He is also the Director of Centre for New Energy Transition Research, Federation University Australia. He has been a Visiting Professor with the Shanghai University of Electrical Power, Shanghai, China. His current research interests include IoT, condition monitoring of transformers, wind energy conversion, and smart power systems.

Dr. Islam was the recipient of the Dean's medallion for research at Curtin University in 1999.

Apurv Kumar received the Ph.D. degree in mechanical engineering from Deakin University, Victoria, Geelong, Australia, in 2015, specialising in modeling and experimental multiphase flow for industrial and natural phenomenon.

He is a Lecturer in mechanical engineering with the Centre for New Energy Transition, Federation University Australia, Ballarat, Australia. He has worked with CSIRO, Newcastle, Australia, and The Australian National University, Canberra, Australia, on a variety of multiphase flow projects. He holds a joint patent with CSIRO and Sandia National Laboratory and is an emerging leader in multiphase flow. He is currently involved with projects concerning multiphase flows like aerosol charging in atmospheric and industrial flows, waste to energy, and wealth projects.